RSC Advances

ROYAL SOCIETY OF CHEMISTRY

www.rsc.org/advances

RSC Advances

COMMUNICATION

Solvothermal Synthesis of MoS_2 Nanospheres in DMF-Water Mixed Solvents and Their Catalytic Activity in Hydrocracking of Diphenylmethane

Received 00th January 20xx,
Accepted 00th January 20xx

DOI: 10.1039/x0xx00000x

www.rsc.org/

Hui Du,[a] Dong Liu,*[a] Min Li,[a] Raja L. AL Otaibi,*[b] Renqing Lv [c] and Yadong Zhang [a]

MoS_2 nanospheres were successfully prepared *via* solvothermal process assisted by 1-ehtyl-3-methylimidazolium bromide ([EMIM]Br) in a mixed solvent of DMF-water. A probable [EMIM]Br aggregation in different mixed solvents and the formation mechanism of MoS_2 nanospheres were presented. Additionally, the MoS_2 nanospheres delivered a high catalytic activity in the hydrocracking of diphenylmethane.

Molybdenum disulfide (MoS_2) with layer and hexagonal structure was wildly used as catalyst,[1] solid lubricant,[2] electrode,[3] and hydrogen storage media,[4] etc. As a catalyst, the layered anisotropic structure of MoS_2 provides massive "edge area" where the catalytic interaction of reactants with MoS_2 edges and defects occurs.[5,6] During the past decades, a variety of catalysts based on MoS_2 were wildly used in the catalytic processes such as the hydrocracking and hydrodesulfurization of petroleum,[7,8] the hydrodeoxygenation of bio-oil,[9] and the production of chemicals.[10,11] Compared with supported catalysts, the unsupported catalysts have the advantages of high dispersion and avoiding pore-plugging problem in residue hydrocracking process. As a consequence, dispersed MoS_2 catalysts have been extensive employed in ENI-EST, SOC, and $(HC)_3$ CASH hydrorefining technologies of residue.[12-14]

MoS_2 with different micro/nano structures have been synthesized through multiple methods, such as solvo-hydrothermal method,[15-17] sonochemical method,[18,19] chemical vapor deposition,[20,21] chemical solution route,[22] microwave synthesis,[23] and thermal sulfurization method.[24] It is well known that solvo-hydrothermal approach was an effective and simple way to prepare micro/nanostructured materials at low temperature.[25] In recent years, ionic liquids (ILs) were used as templates in hydrothermal synthesis of various micro/nano-structured inorganic materials.[16,26,27] Ma et al. obtained MoS_2 microspheres with average diameter about 2.1 μm *via* hydrothermal method assisted by [BMIM][BF_4].[16] Hollow MoS_2 microspheres with diameter ranging from 1.8 μm to 2.1 μm were prepared in [BMIM]Cl/water emulsions.[28] In the same ionic liquids/water medium, hollow vesicle-like MoS_2 microspheres (1-2μm) were synthesized with $(NH_4)_2MoS_4$ as precursor and hydrazine hydrate as reductant.[29] However, to our knowledge, there were no reports on the preparation of MoS_2 nanospheres through solvo-hydrothermal route assisted by ionic liquid.

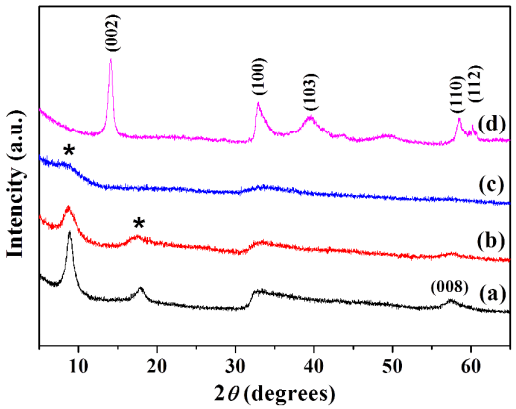

Fig. 1 XRD patterns of MoS_2 samples synthesized at 200 °C for 24h. (a) V_1/V_2 (DMF/water) = 0/9; (b) V_1/V_2 = 3/6; (c) V_1/V_2 = 5/4; and (d) after annealing of (b) in the mixed atmosphere of N_2/H_2 (9/1, v/v) at 700 °C for 2 h. * shifted peaks of (002) and (004).

Table 1 FWHM of the main peaks of MoS_2 samples synthesized in different solvents.

V_1/V_2 (DMF/water)	FWHM	
	(002)	(004)
0/9	0.47°	0.40°
3/6	0.94°	1.16°
5/4	1.87°	2.38°

[a] State Key Laboratory of Heavy Oil Processing, China University of Petroleum, Qingdao 266555, Shandong, P. R. China. E-mail: ldongupc@vip.sina.com; Tel: +86-532-86984629
[b] Petrochemical Research Institute, P.O. Box 6086 Riyadh 11442, King Abdulaziz City for Science and Technology, Kingdom of Saudi Arabia. E-mail: raletabi@kacst.edu.sa.
[c] College of Science, China University of Petroleum, Qingdao 266555, Shandong, P. R. China.
Electronic Supplementary Information (ESI) available: Detailed experimental procedures.

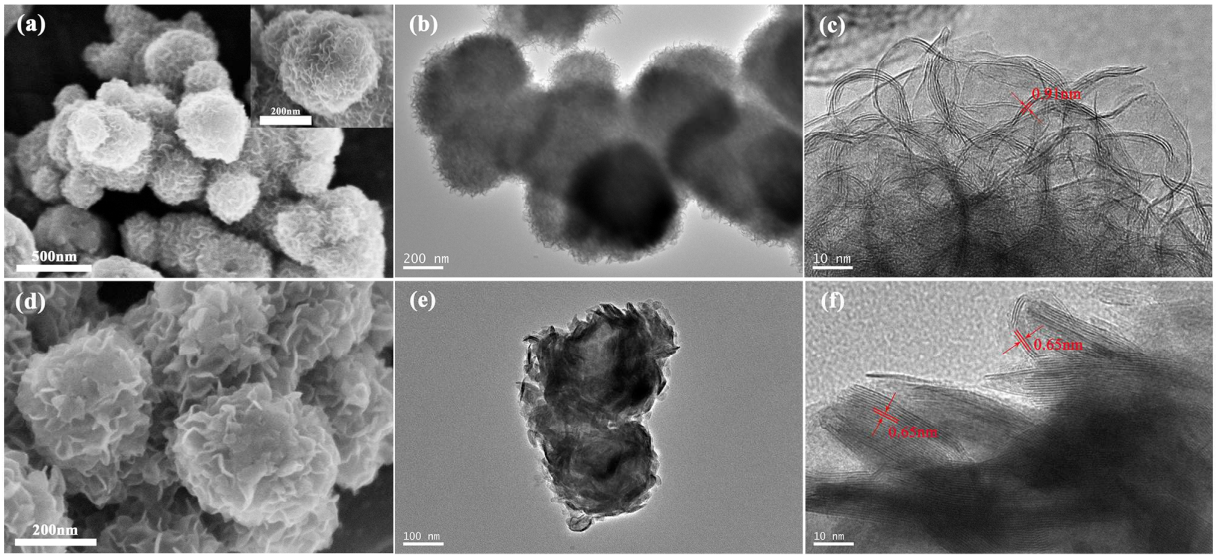

Fig. 2 SEM, TEM and HRTEM images of MoS_2 samples synthesized at 200 °C for 24 h in V_1/V_2 = 3/6. (a-c) before annealing, (d-f) after annealing in the mixed atmosphere of N_2/H_2 (9/1, v/v) at 700 °C for 2 h.

In this research, we present a solvothermal route for the synthesis of MoS_2 nanospheres using a small molecule ionic liquid (1-ethyl-3-methylimidazolium bromide, [EMIM]Br) as template in dimethyl formamide (DMF)-water mixed solvents. A probable [EMIM]Br aggregation in different mixed solvents and the formation mechanism of MoS_2 nanospheres were presented. Additionally, the catalytic activity of as-prepared MoS_2 products in diphenylmethane hydrocracking were investigated.

Detailed experiments from the ionic liquid-assisted solvothermal synthesis of MoS_2 products in DMF-water mixed solvents to their catalytic activity in hydrocracking of diphenylmethane are described in the ESI. XRD patterns of the as-prepared MoS_2 products are demonstrated in Fig. 1. The major diffraction peaks can be indexed to the hexagonal 2H MoS_2 (JCPDS 37-1492). As shown in Fig. 1a-c, the absence of a relative strong diffraction peak at around 2ϑ = 14° (002) reveals that the well-stacked layered structure of MoS_2 did not form during solvothermal process. Meanwhile, the diffraction peaks at 2ϑ = 8.6° and 17.6° are considered to be the (002) and (004) peaks shifting to lower angle range, which has been confirmed by other researchers.[17,29] This is a consequence of the enlarged interlayer spacing caused by the ILs between MoS_2 layers. Comparing with Fig. 1a, the weak peaks in Fig. 1b and c show that the crystallinity of MoS_2 products becomes poor with the presence of DMF. After annealing at 700 °C for 2 h in the mixed atmosphere of N_2/H_2 (9/1, v/v), the MoS_2 products exhibit a strong diffraction peak at 2ϑ = 14.2° (Fig. 1d), implying that the crystallinity of MoS_2 products is improved by annealing.

The morphology and structure of MoS_2 nanospheres, synthesized in mixed solvents of V_1/V_2 = 3/6, before and after annealing were characterized by SEM and TEM. Fig. 2a and b show that the MoS_2 products are nanospheres with the mean diameter of 400 nm. The MoS_2 nanospheres with rough surface are constituted by numerous petal shaped nanoflakes, which can be seen from the clear view of MoS_2 nanosphere in Fig. 2a. From the BET measurement, the specific surface area of MoS_2 nanospheres is 67.9 $m^2 \cdot g^{-1}$. In addition, the HRTEM image (Fig. 2c) clear reveals that the MoS_2 nanoflakes were poorly stacked with fewer layers (3-8 layers) and the average spacing of MoS_2 layers is about 0.91 nm. ILs, inside MoS_2 nanospheres and between MoS_2 layers, would be vanished during annealing at 700 °C. Therefore, the MoS_2 nanospheres become irregular in shape, and the size decreases to 300-400 nm (as shown in Fig. 2d and e). Fig. 2f shows that the petal shaped MoS_2 nanoflakes straightened by annealing, and the number of layers in each flake increases to dozens with a characteristic MoS_2 layer spacing of 0.65 nm (002). The HRTEM results are consistent with the XRD patterns.

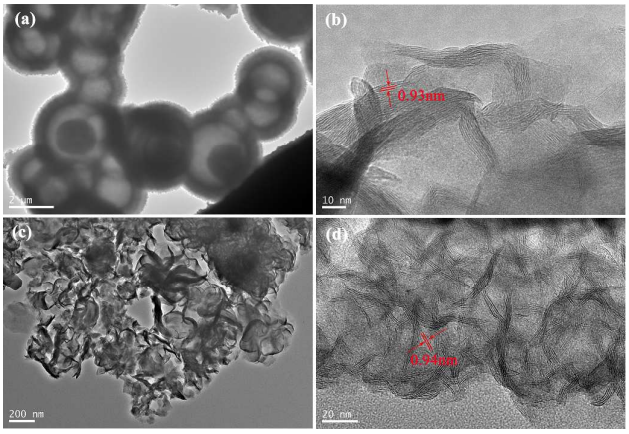

Fig. 3 TEM and HRTEM images of as prepared MoS_2 samples synthesized in V_1/V_2 (DMF/water) = 0/9 (a,b), V_1/V_2 = 5/4 (c,d).

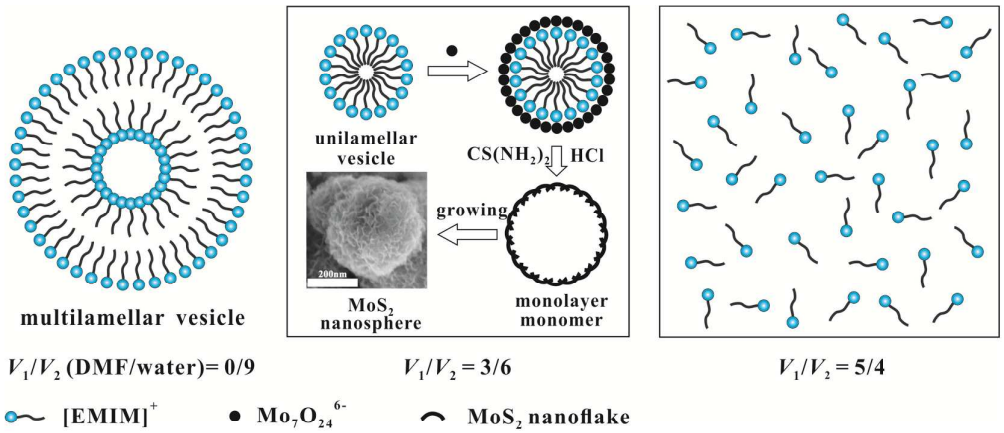

Scheme 1. Schematic illustration of ILs aggregation in different solvents and the formation mechanism of MoS_2 nanospheres synthesized in V_1/V_2 = 3/6.

The ratio of DMF to water plays a significant influence on the morphology of MoS_2 products. As shown in Fig. 3a, the hollow MoS_2 microspheres with diameter of 1.7-3.8 μm were synthesized in the absence of DMF. However, the irregular and agglomerated MoS_2 nanoflakes were obtained in the mixed solvents of V_1/V_2 = 5/4 (Fig. 3c). Compared with the nanoflakes in MoS_2 nanospheres (Fig. 2c), the shape of MoS_2 nanoflakes (Fig. 3d) grew straighter during the solvo-hydrothermal process. The specific surface areas of the hollow MoS_2 microspheres and MoS_2 nanoflakes are 35.1 $m^2 \cdot g^{-1}$ and 49.7 $m^2 \cdot g^{-1}$, respectively. Besides, both the two products in Fig. 3 were poorly stacked with the average spacing of MoS_2 layers greater than 0.9 nm. The full width of half maximum (FWHM) of the main peaks of MoS_2 samples synthesized in different solvents are listed in Table 1. The FWHM values of (002) and (004) reflections increase with increasing the DMF content of mixed solvents. The smallest FWHM value implies the largest crystalline grain of MoS_2 samples synthesized without DMF. As can be seen from the HRTEM images of MoS_2 samples, the flakes in MoS_2 samples synthesized without DMF show more straight structure and MoS_2 layers.

According to literature,[22] the reaction involved in the solvothermal synthesis process was shown as follows:

$$4\ (NH_4)_6Mo_7O_{24}\cdot + 63\ CS(NH_2)_2 + 136\ HCl + 58\ H_2O \rightarrow 28\ MoS_2 + 7\ (NH_4)_2SO_4 + 136\ NH_4Cl + 63\ CO_2$$

It has been reported that ILs act as template in solvo-hydrothermal synthesis of MoS_2.[16,28,29] $[EMIM]^+$ could form vesicles in certain solvent under proper conditions. Then, $Mo_7O_{24}^{6-}$ anions adsorb on the vesicle surface through electrostatic attraction,[30] which react with the H_2S in situ produced by hydrolysis of $CS(NH_2)_2$. Based on the experimental results, the probable ILs aggregation in different solvents and the formation mechanism of MoS_2 nanospheres synthesized in V_1/V_2 = 3/6 is presented in Scheme 1. ILs could form multilamellar vesicles with diameter of a few micrometres in pure water. With the gradually addition of DMF, the multilamellar vesicles break because of higher energy, then small multilamellar vesicles or unilamellar vesicles are formed to obtain a low energy state.[31] MoS_2 nanospheres generated gradually on the surface of ILs vesicles (V_1/V_2 = 3/6). However, if the addition of DMF continues, the stable aggregation structure of ILs could not form in the mixed solution (V_1/V_2 = 5/4).

Table 2 shows the results of DPM hydrocracking in the presence of different MoS_2 products at various temperatures. It can be seen that DPM barely hydrocracked when the reaction was performed at

Table 2 Results of DPM hydrocracking in the presence of different MoS_2 catalysts under the initial hydrogen pressure of 5.0 MPa at different temperatures for 1 h.

Catalyst	Temperature (°C)	Conversion of DPM (%)	Selectivity (mol%)			
			Benzene	Toluene	BCH	DHM
None	450	0.7	100	99.9	0	0
MoS_2 microsphere	350	15.1	75.3	75.3	23.8	0.9
	400	39.6	88.6	88.6	9.7	1.7
	450	52.5	90.1	90.1	7.3	2.6
MoS_2 nanosphere	350	18.9	69.5	69.5	29.4	1.1
	400	51.5	83.1	83.2	13.9	2.9
	450	72.8	83.8	83.8	10.8	5.4
MoS_2 nanoflake	350	17.8	71.9	71.8	27.4	0.8
	400	48.1	86.2	86.2	11.8	2.0
	450	66.3	87.6	87.5	8.3	4.2

BCH, benzylcyclohexane; DHM, dicyclohexylmethane.

450 °C without catalyst, while all of the MoS_2 products significantly facilitate the conversion of DPM. Under the hydrocracking conditions, the coordinatively unsaturated sites can be readily formed at the edge and corner positions of MoS_2, which are the sites for hydrogen activation.[32] Hydrogen molecules split to yield the hydrogen free-radicals on the coordinatively unsaturated sites, then the produced hydrogen free-radicals addition to the ipso position of DPM to trigger the scission of C_{ar}–C_{alk} bond.[33] Besides, the produced hydrogen free-radicals also can help to saturate the aromatic rings of DPM. Benzene and toluene are the main products of DPM hydrocracking, while small amounts of benzylcyclohexane and dicyclohexylmethane are also identified in the hydrocracked products.

As demonstrated from Table 2, under the same hydrocracking conditions, the order about the conversion of DPM in the presence of different MoS_2 products from high to low is MoS_2 nanosphere, MoS_2 nanoflake, MoS_2 microsphere, which is consistent with the order of specific surface area of the MoS_2 products. MoS_2 with high specific surface area can provide more coordinatively unsaturated sites and yield more hydrogen free-radicals to participate the reaction. The MoS_2 nanosphere delivered a higher catalytic activity in DPM hydrocracking than FeS_2 catalyst[33] and MoS_2 catalyst produced by water-soluble Mo precursor.[34] Liu et al. used the ratio of gross products of hydrosaturation and DPM conversion to describe the "hydrogenation activity" of the catalyst.[34] Therefore, the prepared MoS_2 nanosphere present the higher hydrogenation activity than MoS_2 microsphere and MoS_2 nanoflake. Moreover, the catalytic activity difference between MoS_2 nanosphere and nanoflake was enhanced by high temperature. Table 2 also shows that the conversion of DPM increased with increasing the reaction temperature with the presence of same catalyst. The fact indicates that high temperature facilitates the formation of hydrogen free-radicals to participate DPM conversion.

The selectivity results of DPM hydrocracking in Table 2 shows that the percent of scission products (benzene and toluene) greatly increased with the increase temperature from 350 °C to 400 °C, while it increased hardly when the temperature increased from 400 °C to 450 °C. Whereas the percent of DHM remained increasing with the increase temperature. The results revealed that the scission of C_{ar}–C_{alk} bond dominates the reaction at high temperature, meanwhile the hydrogenation saturation abilities of MoS_2 products were enhanced by high temperature. Additionally, at the same temperature, DPM conversion with MoS_2 nanosphere showed higher yields of BCH and DHM, which indicated that the hydrogenation saturation ability of MoS_2 nanosphere was higher than MoS_2 nanoflake and MoS_2 microsphere.

Conclusions

In summary, MoS_2 nanospheres with average diameter of 400 nm and specific surface area of 67.9 $m^2 \cdot g^{-1}$ were successfully prepared *via* solvothermal process assisted by [EMIM]Br in a mixed solvent of DMF-water (V_1/V_2 = 3/6) at 200 °C for 24h. The ratio of DMF to water has a significant effect on the size and morphology of MoS_2 products. The strategy described here might be extended to other transition metal sulfide nano-materials. Additionally, the MoS_2 nanospheres delivered a high catalytic activity in the hydrocracking of diphenylmethane. The scission of C_{ar}–C_{alk} bond dominates the DPM conversion at high temperature. Meanwhile, the hydrogenation saturation abilities of MoS_2 products were enhanced by high temperature, which of MoS_2 nanosphere was higher than MoS_2 nanoflake and MoS_2 microsphere at same temperature.

Acknowledgement

This work was financially supported by the National Natural Science Foundation of China (21176259), Shandong Provincial Natural Science Foundation, China (ZR2015BM003) and the Fundamental Research Funds for the Central Universities (15CX05009A).

Notes and references

1 J. Chen, S. Li, Q. Xu and K. Tanaka, *Chem. Commun.,* 2002, **16**, 1722-1723.
2 L. Rapoport, Y. Bilik, Y. Feldman, M. Homyonfer, S.R. Cohen and R.Tenne, *Nature*, 1997, **387**, 791-793.
3 Q. Wang and J. Li, *J. Phys. Chem. C*, 2007, **111**, 1675-1682.
4 J. Chen, N. Kuriyama, H. Yuan, H.T. Takeshita and T. Sakai, *J. Am. Chem. Soc.,* 2001, **123**, 11813-11814.
5 S.J. Tauster, T.A. Percoraro, and R.R. Chianelli, *J. Catal.*, 1980, **63**, 515-519.
6 R.R. Chianelli, A.F. Ruppert, S.K. Behal, B.H. Kear, A. Wold and R. Kershaw, *J. Catal.*, 1985, **92**, 56-63.
7 C. T. Tye and K. J. Smith, *Catal. Lett.*, 2004, **95**, 203-209.
8 C. T. Tye and K. J. Smith, *Catal. Today*, 2006, **116**, 461-468.
9 P. M. Mortensen, J.-D. Grunwaldt, P.A. Jensen, K.G. Knudsen and A.D. Jensen, *Appl. Catal. A-Gen.*, 2011, **407**, 1-19.
10 V. P. Santos, B. van der Linden, A. Chojecki, G. Budroni, S. Corthals, H. Shibata, G. R. Meima, F. Kapteijn, M. Makkee, and J. Gascon, *ACS Catal.,* 2013, **3***,* 1634-1637.
11 M. Soto-Puente, M. Del Valle, Eric Flores-Aquino, M. Avalos-Borja, S. Fuentes and J. Cruz-Reyes, *Catal. Lett.*, 2007, **113**, 170-175.
12 G. Bellussi, G. Rispoli, D. Molinari, A. Landoni, P. Pollesel, N. Panariti and E. Montanari, *Catal. Sci. Techn.*, 2013, **3**, 176-182.
13 G. Bellussi, G. Rispoli, A. Landoni, R. Millini, D. Molinari, E. Montanari and P. Pollesel, *J. Catal.*, 2013, **308**: 189-200.
14 R.R. Chianelli, M. H. Siadati, M. P. De la Rosa, G. Berhault, J. P. Wilcoxon, R. Bearden Jr. and B. L. Abrams, *Catal. Rev.*, 2006, **48**, 1-41.
15 D. Wang, Z. Pan, Z. Wu, Z. Wang and Z. Liu, *J. Power. Sources*., 2014, **264**, 229-234.
16 L. Ma, W.-X. Chen, H. Li, Y.-F. Zheng and Z.-D. Xu, *Mater. Lett.*, 2008, **62**, 797-799.
17 L. Ma, L.M. Xu, X.P. Zhou and X.Y. Xu, *Mater. Lett.*, 2014, **132**, 291-294.
18 D. Mahajan, C. L. Marshall, N. Castagnola and J. C. Hanson, *Appl. Catal. A-Gen.*, 2004, **258**, 83-91.
19 N. Savjani, E. A. Lewis, R. A. D. Pattrick, S. J. Haigh and P. O'Brien, *RSC Adv.*, 2014, **4**, 35609-35613.
20 Y.H. Lee, X.Q. Zhang, W. Zhang, M.T. Chang, C.T. Lin, K.D. Chang, Y.C. Yu, J. T.W. Wang, C.S. Chang, L.J. Li and T.W. Lin, *Adv. Mater*., 2012, **24**, 2320-2325.
21 J. Wang, L. Chen, W. Lu, M. Zeng, L. Tan, F. Ren, C. Jiang and L. Fu, *RSC Adv.*, 2015, **5**, 4364-4367.
22 H. Liao, Y. Wang, S. Zhang and Y. Qian, *Chem. Mater.*, 2001, **13**, 6-8.
23 D. Vollath and D.V. Szabó, *Mater. Lett.*, 1998, **35**, 236-244.

24 M. Remškar, A. Mrzel, M. Viršek and A. Jesih, *Adv. Mater.*, 2007, **19**, 4276-4278.
25 M. Rajamathi and R. Seshadri, *Current Opinion in Solid State and Materials Science*, 2002, **6**, 337-345.
26 T. Wang, H. Kaper, M. Antonietti and B. Smarsly, *Langmuir*, 2007, **23**, 1489-1495.
27 T. Zhang, H. Guo and Y. M.Qiao, *J. Lumin.*, 2009, **129**, 861-866.
28 H. Luo, C. Xu, D. Zou, L. Wang and T. Ying, *Mater. Lett.*, 2008, **62**, 3558-3560.
29 N. Li, Y. Chai, Y. Li, Z. Tang, B. Dong, Y. Liu and C. Liu, *Mater. Lett.*, 2012, **66**, 236-238.
30 H. Li, W. Li, L. Ma, W. Chen and J. Wang, *J. Alloy. Compd.*, 2009, **471**, 442-447.
31 Y. Shen, H. Hoffmann and J.Hao, *Langmuir*, 2009, **25**, 10540-10547.
32 E. Furimsky, Catalysts for upgrading heavy petroleum feeds. Elsevier, 2007.
33 X. Y. Wei, E. Ogata, Z. M. Zong and E. Niki, *Energ. Fuel.*, 1992, **6**, 868-869.
34 D. Liu, X. Kong, M. Li and G. Que, *Energ. Fuel.*, 2009, **23**, 958-961.